

# Coordination Area to Prevent Interference from LMDS Transmitters Operating in the 25.7-GHz Band in Areas around the Robledo DSN Stations in Spain

Christian Ho\*

The Local Multipoint Distribution Service (LMDS) is a broadband wireless point-to-multipoint (P-MP) communication system operating in the frequency band between 24.5 and 26.5 GHz. The LMDS systems can cause potential interference to the Deep Space Network (DSN) stations in Robledo by propagating over the horizon and over the intervening terrain. This article assesses the potential interference to the Robledo DSN antennas from the LMDS emitters operating around the Madrid area and develops a coordination contour for planning future LMDS development in areas surrounding the Robledo DSN antennas.

## I. Background

The Local Multipoint Distribution Service (LMDS) is a broadband wireless point-to-multipoint (P-MP) communication system operating in the frequency band between 24.5 and 26.5 GHz that can be used to provide digital two-way voice, data, Internet, and video services. However, the LMDS deployment in the area around Madrid, Spain can cause potential interference to the Deep Space Network (DSN) stations in Robledo because the DSN will operate in the 25.5- to 27.0-GHz frequency band to support lunar and Lagrangian orbit missions. Although there is no direct line-of-sight in general between the LMDS transmitters and the DSN antennas at Robledo, emissions from the LMDS transmitters can be received by the DSN antennas through anomalous propagation modes, and the emissions may exceed the protection criteria established by the International Telecommunications Union (ITU) for the protection of the Space Research Service (SRS) in this band. The study described here estimates the interference levels and suggests a coordination area to protect the DSN antennas from harmful interference from LMDS transmitters operating in areas around the Robledo DSN site.

## II. A Brief Description of the LMDS Systems and Characteristics

To perform this study, certain parameters of the LMDS systems are needed. SETSI (Spanish Secretary of State for Telecommunications and Information Society) provided the character-

---

\* Communication Architectures and Research Section.

The research described in this publication was carried out by the Jet Propulsion Laboratory, California Institute of Technology, under a contract with the National Aeronautics and Space Administration.

istics of the LMDS systems deployed around Madrid in a NASA/SETSI document.<sup>1</sup> Information from this document forms the basis of this study and is summarized below.

The LMDS systems in Spain have the following specifications: The point-to-multipoint (P-MP) communication system operates in the 24.549- to 24.717-GHz band for downlinks and in the 25.557- to 25.725-GHz band for uplinks. The uplinks that are of interest to us are from subscribers (terminal stations) to the base station. Typically, each 56-MHz downlink channel is paired with eight 7-MHz uplink carriers that provide 10.75 Mbps each on the air. Each downlink channel of 56 MHz is used by two 28-MHz carriers, and each of these carriers is paired with four 7-MHz uplink channels. The frequency spectrum for this system is shown in Figure 1. A typical cell consists of four 90-deg sectors. As shown in Figure 2, two adjacent sectors use different frequencies, while two opposite sectors use the same frequency but with opposite polarizations.

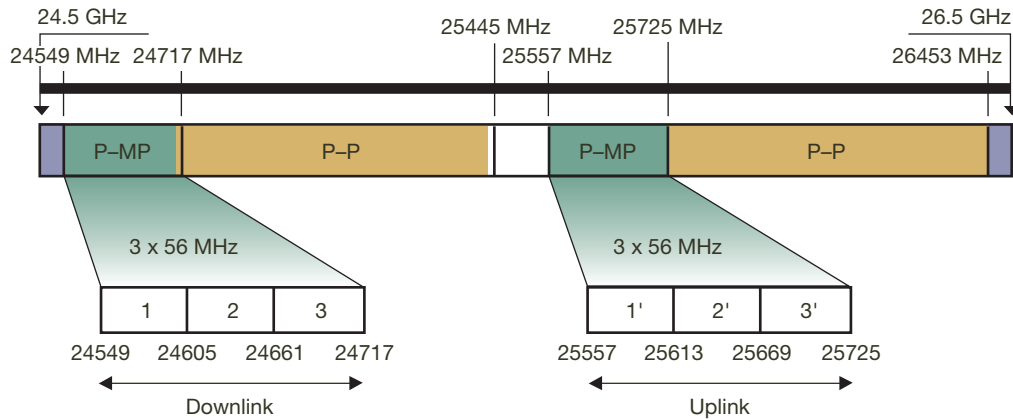


**Figure 1. Frequency spectrum for the LMDS systems deployed around Madrid in Spain. Transmission from a terminal station to a base station (uplink) will interfere with the DSN receiving station at Robledo.**

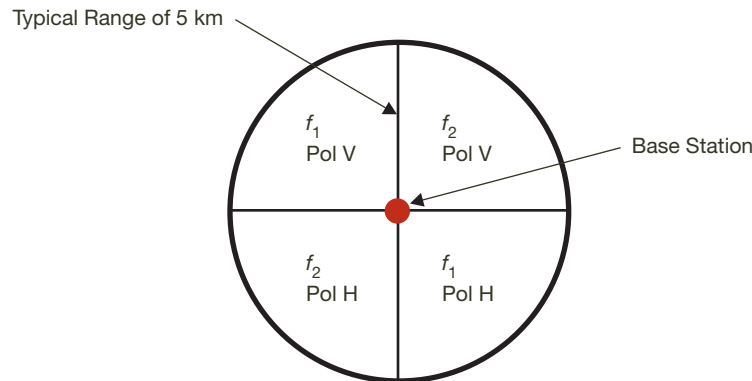


**Figure 2. An LMDS cell that consists of a base station and a number of terminal stations. The cell is divided into four 90-deg sectors to achieve frequency reuse.**

<sup>1</sup> Personal communication, Benito Gutierrez-Luaces, July 27, 2006; NASA/SETSI document provided by Carlos Carrascal, June 15, 2007.

The subscriber terminal unit transmits a 7-MHz carrier with 14 dBm power (−16 dBW) to a subscriber antenna of approximately 35 dBi gain. The cell size for a typical base station is 5 km. The typical location of a base station is on top of the hills or tall buildings. The subscriber antennas thus generally point slightly up (from 0 to 3 deg).

### III. Study Approach and Assumptions

The DSN receiving station at Robledo will use the 25.5- to 27.0-GHz frequency band to support downlinks from lunar and Lagrangian orbit missions. Thus, it has an overlap in the frequency between 25.557 and 25.725 GHz with the LMDS uplink. In this article, we first estimate the interference level received by the Robledo DSN antennas from one LMDS cell located at a given azimuth angle, and then compare that level with the space research protection criterion established by the ITU for this band. From this comparison, the necessary coordination distance to prevent harmful interference to the DSN in that azimuth direction is determined. The process is repeated for all azimuth angles to obtain a complete coordination contour around the Robledo DSN site. A number of simplifying assumptions are used.

### IV. Analysis of Interference from Emitters of One Cell in a Given Azimuth Direction

Table 1 shows a sample link analysis. We have assumed that the interference is from one single LMDS cell in a given azimuth direction. There may be more than one transmitter in that cell contributing to the interference (to be discussed later). Interference from emitters in other cells, in the same azimuth direction or otherwise, is not considered. The key parameters in the table are described below.

**Table 1. Link table for LMDS interference analysis.**

Parameter	Symbol	Value	Unit	Value	Unit in dB
Transmitting frequency	$f$	25.7	GHz		
Transmitter power per carrier	$T_x$			−16	dB(W)
Transmitter antenna boresight gain	$G_t$			35	dBi
Top 1 percent antenna gain				31	dBi
EIRP for each carrier at 1 percent				15	dB(W)
Transmitting data rate		10.75	Mbps		
Transmitting bandwidth	$B$	7	MHz	68.5	dB(Hz)
Transmitter EIRP PSD	$EIRP_{PSD}$			−53.5	dB(W/Hz)
Transmitter cell range		5	km		
DSN receiver antenna gain	$G_r$			variable	dBi
DSN receiver system noise temperature when pointed to the Moon	$T_{sys}$	350	K		
DSN receiver noise spectral density	$N_0$			−203.1	dB(W/Hz)
Allowed $I_0 N_0$				−6	dB
Interference threshold	$I_0$			−209.1	dB(W/Hz)
Propagation loss required for one transmitter	$L_{req}$			$155.6 + G_r$	dB

### A. Effective Transmitter Antenna Gain

For LMDS transmitter within about 50 km from the Robledo station in the east and south directions, the dominating propagation mode is the diffraction mode (to be discussed later). The interference level in this case is a function of the distance and the effective gains of both the transmitting antenna and the receiving antenna in the transmitter-to-DSN direction. The effective gain for a given transmitter antenna is its gain in the direction of the DSN antennas in Robledo. The maximum antenna gain is 35 dBi. This gain is reduced by an amount determined by the off-axis angle, i.e., the angle between the boresight of the transmitter antenna and the direction to the DSN. The effective gain of the receiving antenna is the gain of the DSN antenna in the direction of the interference along the transmitter-to-DSN direction (to be discussed in more detail later).

In general, the effective gain for a given transmitter is determined by its pointing direction in elevation and azimuth. As stated before, the subscriber antennas generally point slightly up towards the base station, which is typically located on top of a hill or a tall building. For the diffraction mode, interference from the LMDS transmitters in a given azimuth direction is assumed to be coming from the top of the intervening hills in that direction. The effective gain can thus be assumed to be solely determined by the pointing of the transmitting antenna in the azimuth direction.

As previously mentioned, there are two transmitters using the same 7-MHz frequency channel with opposite polarizations in each cell. Therefore, for a given frequency and polarization, there will be only one LMDS transmitter in each cell contributing to interference to the DSN. At any time we only see one LMDS transmitter with its antenna pointed towards the DSN direction. Figure 3 is a reference radiation pattern based on ITU-R recommenda-

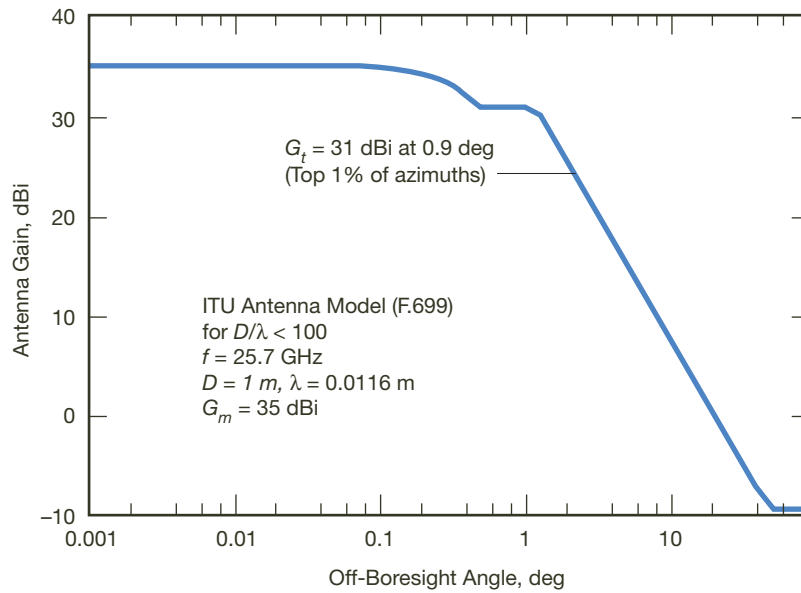


**Figure 3. Antenna gain model for the LMDS transmitter antenna based on ITU F.669 model for a small antenna (with  $D/\lambda < 100$ ). At the top 1.0 percent of azimuth distribution, the antenna has a gain of 31 dBi.**

tion F.699. Under the assumption that the off-axis angle is uniformly distributed in  $(-90, 90 \text{ deg})$ , the effective antenna gain for a 99 percent confidence level is calculated below:

$$\begin{aligned}\text{Minimum off-axis angle} &= 90 \times (100 \text{ percent} - 99 \text{ percent}) = 0.9 \text{ deg} \\ \text{Effective transmitting antenna gain} &= G_t (0.9 \text{ deg}) = 31 \text{ dBi}\end{aligned}$$

where  $G_t$  is the transmitter antenna gain. The gain in the direction to the DSN site is less than or equal to 31 dBi for 99 percent of the time. Only during 1 percent of the time would the gain exceed 31 dBi.

#### B. Transmitter EIRP Power Spectral Density

Using the effective transmitting antenna gain of 31 dBi and a bandwidth of 7 MHz, and assuming that only one transmitter in each cell could contribute to interference to the DSN, the transmitter's effective isotropic radiated power (EIRP) spectral density (PSD) can be calculated as follows:

$$EIRP_{PSD} = 31 \text{ dBi} - 16 \text{ dBW} - 68.5 \text{ dB (Hz)} = -53.5 \text{ dB (W/Hz)} \quad (1)$$

#### C. Applicable SRS Protection Criterion

The SRS protection criterion established by the ITU for the frequency band of interest is  $I_0/N_0 = -6 \text{ dB}$  for 99.9 percent of the time, where

$$\begin{aligned}I_0 &= \text{Interference spectral density, dB(W/Hz)} \\ N_0 &= \text{Receiver noise spectral density, dB(W/Hz)} = k_B T_{sys}\end{aligned}$$

where  $k_B$  is the Boltzmann constant, while  $T_{sys}$  is system noise temperature.

#### D. Receiver System Noise Temperature

When the DSN antenna is tracking a lunar mission on or near the Moon, the background noise from the Moon contributes a significant part to the total system noise temperature. Based on existing link design for lunar mission operating in the 25.5- to 27-GHz band, the total system noise temperature is 350 K.<sup>2</sup> (The system noise temperature for Lagrangian orbit missions is discussed in Appendix A).

#### E. Maximum Allowed Interference Spectral Density and Required Propagation Loss

The DSN receiver system noise when it points to the Moon is therefore

$$\begin{aligned}N_0 &= k_B T_{sys} \\ N_0 &= -228.6 + 10 \log_{10}(350) = -203.1 \text{ dB (W/Hz)}\end{aligned} \quad (2)$$

---

<sup>2</sup> Provided by Sal Kayalar. Also see the 2005 IEEE Aerospace Conference paper by G. K. Noreen et al. [1]

Based on a protection criterion of  $-6$  dB of  $I_0/N_0$ , the maximum allowed interference spectral density is

$$I_0 = -209.1 \text{ dB (WHz)}$$

The required minimum propagation loss needed to reduce the interference to not exceed the allowable level is

$$L_{req} = EIRP_{PSD} + G_r - I_0 = -53.5 + G_r + 209.1 = 155.6 + G_r \text{ (dB)} \quad (3)$$

where  $G_r$  is the effective gain of the receiving DSN antenna, i.e., the gain in the direction of the interference. For a different receiving antenna gain  $G_r$ , there is a different  $L_{req}$  and consequently a different coordination distance.

#### F. Effective Gain of the DSN Antenna

In order to determine the amount of propagation loss, it is necessary to determine the effective gain of the receiving DSN antenna in the direction of the interference. This gain is a function of the separation angle between the antenna boresight and the interference path. The DSN receiving antennas at Robledo are surrounded by hills. There is no direct line of sight in general between the DSN and the LMDS transmitters in the Madrid area. However, emissions from the LMDS transmitters can propagate trans-horizontally over the intervening hills and be received by the DSN antennas. For most azimuth directions and for close distances, terrain diffraction is the dominant mode for interference propagation. For a given azimuth direction, the interference can be assumed to come from the top of the intervening hills in that direction. Consequently, the effective receiving antenna gain is determined by the separation angle between the DSN antenna boresight and the direction from the DSN antenna to the top of the hills along that azimuth direction, as illustrated in Figure 4.

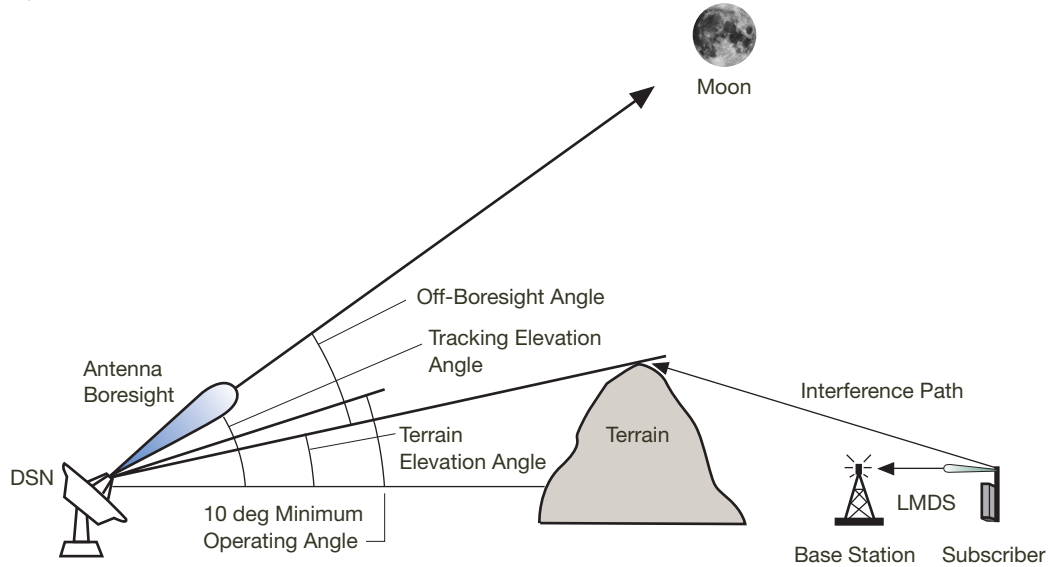


**Figure 4. An illustration of various angles used in this study. Interference from LMDS subscriber stations around Madrid can propagate over the terrain and be received by the DSN station.**

In Figure 4, the DSN antenna tracking a lunar mission at or near the Moon is pointed to a certain elevation angle and azimuth angle. The emissions from an LMDS transmitter located some distance away from the DSN antenna reach the DSN antenna by propagating over the intervening terrain. The terrain elevation angle, the tracking elevation angle, the separation angle, and the minimum operation angle are shown in this figure. The minimum operational angle is the elevation angle at the beginning of the track, which is assumed to be 10 deg for the 25.5- to 27-GHz band.

## V. Coordination Contour

Applying the method discussed in the previous section, we have established the coordination distance (or coordination contour) for azimuth angles ranging from 0 to 360 deg at 1-deg increments. There are two key assumptions in developing the contour:

- (1) There is one LMDS cell in each azimuth direction. The coordination distance for a given azimuth direction is determined by the interference from this cell in that azimuth direction, without considering interferences from cells in other azimuth directions.
- (2) The minimum possible separation angle is used to determine the coordination distance, taking into account the minimum operational elevation angle of 10 deg, the terrain elevation angle, and the minimum tracking elevation angles.

### A. Minimum Separation Angle while Tracking a Lunar Mission

The maximum and minimum elevation angles of the DSN antenna tracking a lunar mission are obtained from a computer simulation based on one year of tracking data. Table 2 lists six sample tracks (each separated by two months) showing the azimuth and elevation

**Table 2. Required propagation losses for six representative lunar tracks.**

Parameters	Case 1	Case 2	Case 3	Case 4	Case 5	Case 6
Sample date	Jan. 1	Mar. 1	May 1	July 1	Sept. 1	Nov. 1
Start of track ( $t_1$ )						
El( $t_1$ )	10.0	10.0	10.0	10.0	10.0	10.0
Az( $t_1$ )	84.1	120.8	133.9	79.3	70.8	117.9
El_terrain at Az( $t_1$ )	7.2	2.9	3.8	6.7	4.5	2.9
Sep. angle $\theta_1$ of El <sub>1</sub> and El <sub>1-ter</sub>	2.8	7.1	6.2	3.3	5.5	7.1
$G_{r1}$ at $\theta_1$ , dB	20.8	10.7	12.2	19.0	13.5	10.7
$L_{req}=155.6+G_{r1}$	176.4	166.3	167.8	174.6	169.1	166.3
End of track ( $t_2$ )						
El( $t_2$ )	10.0	10.0	10.0	10.0	10.0	10.0
Az( $t_2$ )	272.7	236.5	228.6	284.0	286.4	239.2
El_terrain at Az( $t_2$ )	6.0	4.6	4.9	6.5	7.2	4.8
Sep. angle $\theta_2$ of El <sub>2</sub> and El <sub>2-ter</sub>	4.0	5.4	5.1	3.5	2.8	5.2
$G_{r2}$ at $\theta_2$ , dB	16.9	13.7	14.3	18.4	20.8	14.1
$L_{req}=155.6+G_{r2}$	172.5	169.3	169.9	174.0	176.4	169.7

angles during a track from moonrise (from east) to moonset (to west). The maximum and minimum tracking elevation angles are shown in Figure 5 as a function of the azimuth angle. The Moon (or the lunar mission) can appear anywhere within the shaded region. The other two curves in the figure are the terrain-elevation angles (terrain mask) and the assumed minimum operational elevation angle of 10 deg.

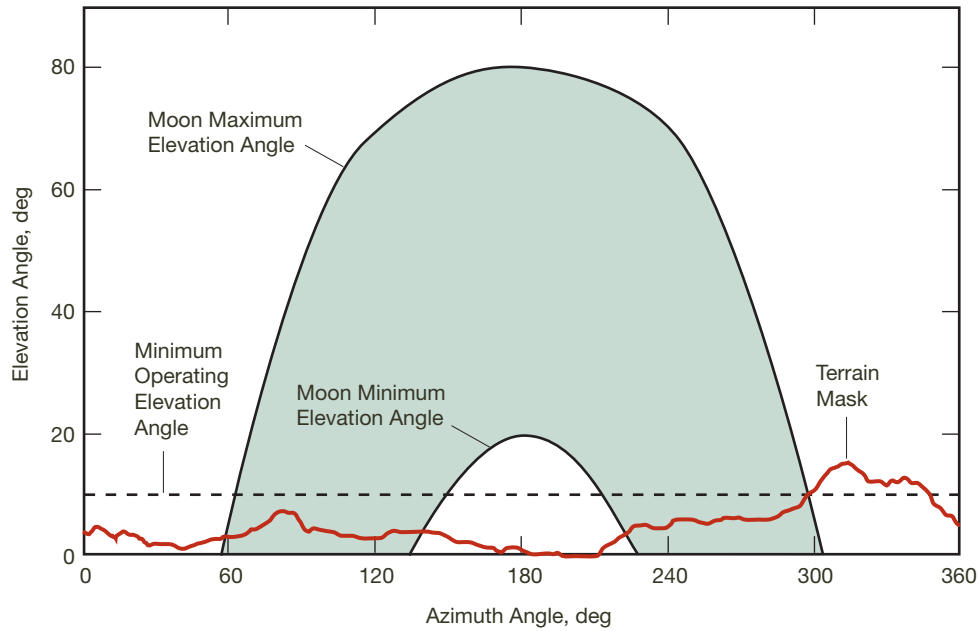


**Figure 5. Maximum and minimum elevation angles for the DSN receiving antenna tracking the Moon. During the year, the Moon rises from the east and sets to the west, but it can appear anywhere within the shaded area. The assumed antenna minimum operating angle (10 deg) and the terrain (terrain mask) elevation angle around the Robledo DSN station for all azimuth directions are also shown.**

The minimum separation angle for each azimuth angle and the effective receiving antenna gain are calculated and shown in Figure 6. The gain is based on the ITU antenna model (F.699) for the 34-m DSN antenna ( $D/\lambda < 100$ ). Because the Moon (or the lunar mission) is below the horizon between 0 to 60 deg and 300 to 360 deg azimuth sectors, as shown in the figure, the receiving antenna gain is assumed to be -10 dBi in those sectors. Between 60 to 140 deg and 220 to 300 deg azimuth sectors, the minimum separation angle is the difference between the terrain angle and minimum operational elevation angle of 10 deg. For the azimuth range between 140 to 220 deg, the minimum separation angle is the difference between the Moon's minimum elevation angle and the terrain elevation angle.

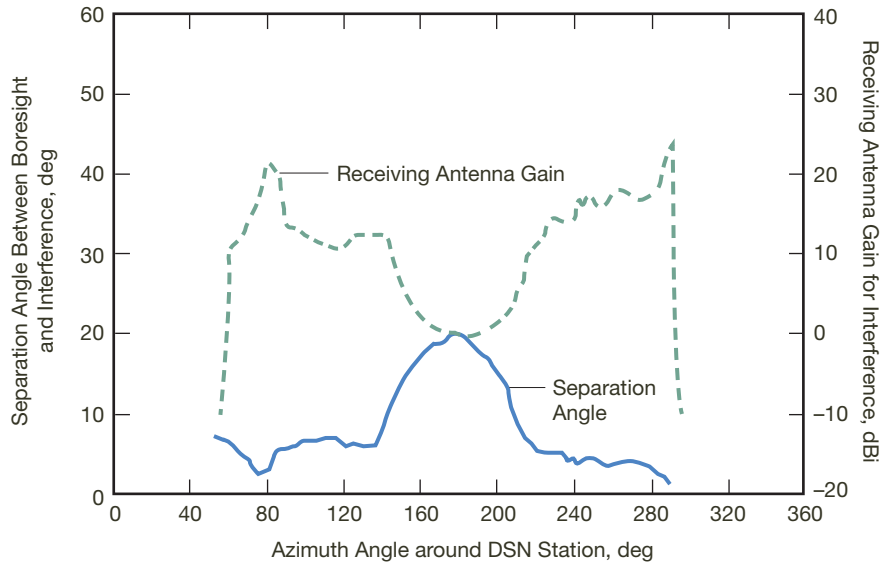


**Figure 6.** The separation (off-boresight) angles between the boresight of the receiving antenna and the direction of interference as a function of azimuth angle around the Robledo DSN station are shown using the left axis and a solid line. The effective antenna gains of the DSN receiving antenna are shown using the right axis and a dotted line. When the azimuth angle is less than 60 deg or greater than 300 deg, the Moon is below the horizon and the receiving antenna gain is  $-10$  dBi.

Using the calculated receiving antenna gains, the required minimum propagation loss defined in Equation (3) is shown in Figure 7. We can see that it only requires 145.6 dB in the northern direction (in the 0 to 60 deg and 300 to 360 deg azimuth sectors), while 150 to 160 dB in the southern direction (150 to 210 deg). In the rest of the azimuth directions, larger losses (160 to 180 dB) are needed. Using this propagation loss curve, a coordination contour can be determined.

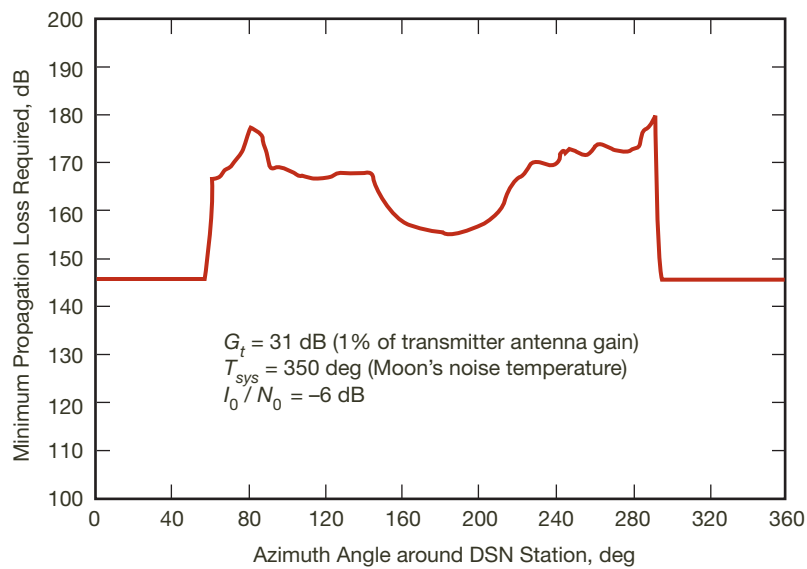


**Figure 7.** Minimum propagation loss required to meet the ITU protection criteria as a function of azimuth angle.

### B. Two-Dimensional Propagation Loss Map and Coordination Contours

Using the Trans-Horizon Interference Propagation Loss (THIPL) computer program and high-resolution terrain data, a propagation loss map (in Figure 8) has been generated for the Madrid–Robledo area for the 26-GHz band and for  $p = 1.0$  percent where  $p$  is the percentage of time when the loss is NOT exceeded. As shown in the map, in the east side of the DSN site is the Madrid metropolitan area where LMDS base stations are being deployed. The planned LMDS base stations are also shown in the figure. Applying the required minimum propagation losses showed in Figure 7, we could define a coordination zone around the Robledo DSN station as marked by a black line in the map. This contour circles an area beyond which a single cell of LMDS transmitters at a given azimuth angle will not interfere with the DSN antenna more than 1.0 percent of the time.

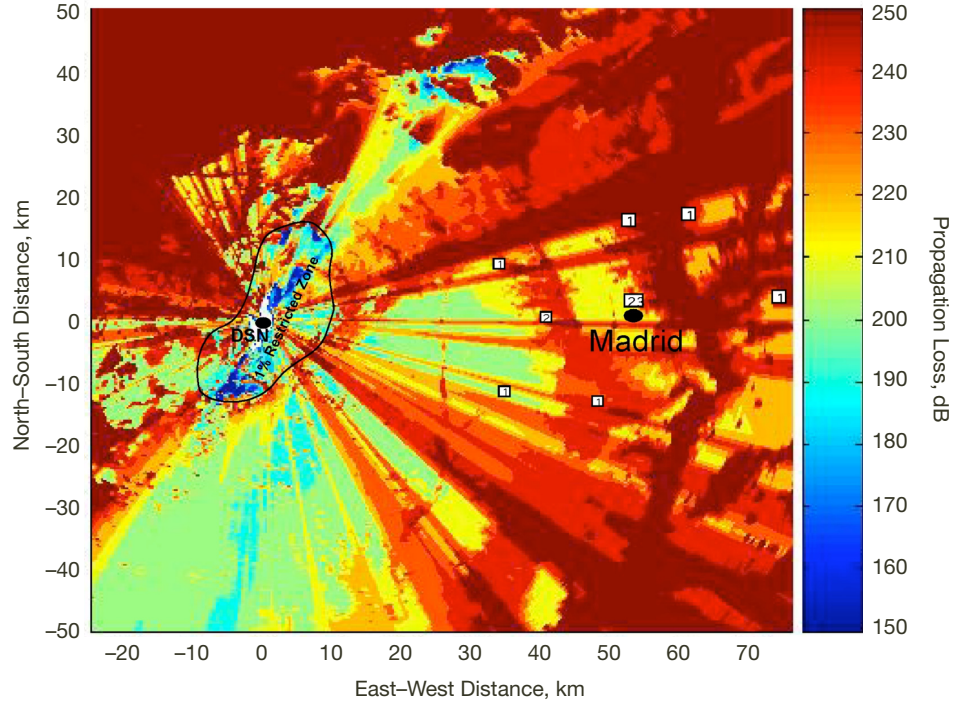


**Figure 8. Propagation loss map with a coordination area around the Robledo DSN site for 1.0 percent of time exceeded. LMDS stations deployed inside this area will cause harmful interference to the Robledo DSN station.**

**There are total 32 existing LMDS cells deployed around Madrid in the east side of the DSN station but outside of the coordination area.**

The contour assumes a minimum separation angle between the boresight of the DSN antenna and the interference path as discussed in Section V.A. This minimum separation angle happens at the beginning or the end of the track when the DSN antenna elevation angle is low. As the DSN antenna elevation angle rises during a track, the separation angle becomes larger, the power level of the interference received by the DSN becomes lower, and the percentage of time ( $p$ ) becomes smaller. The percentage of time ( $p$ ) averaged over the entire track hence will be much smaller than 1.0 percent. The average percentage of time is estimated for six typical tracks in Appendix B.

## VI. LMDS Deployments in Madrid

An expanded map with the LMDS base station deployment pattern in the Madrid metropolitan areas is showed in Figure 9. The coordination zone (for  $p = 1.0$  percent) around Robledo DSN site is also showed in the left side of this map.

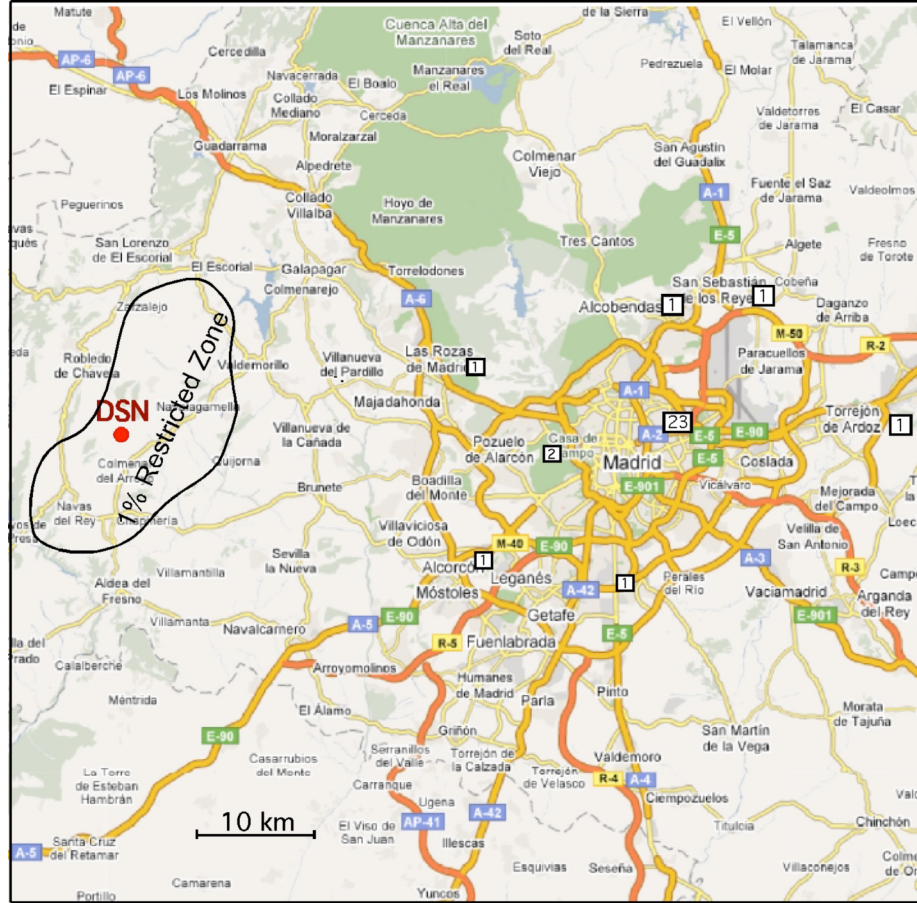


Figure 9. LMDS base station deployment map around the Madrid metropolitan area. On the left side is the coordination area around the DSN site for 1.0 percent of time exceeded. All deployed stations are outside of this area.

Based on information provided by SETSI, 31 base stations have been deployed in the Madrid metropolitan area. In Table 3, we have listed the numbers of LMDS base stations deployed at each city around the Madrid area, the terrain elevation angles seen by the DSN in the direction of that city, and the off-boresight (separation) angles of the receiving antenna and the corresponding antenna gains. We can see that the receiving antenna gains in the direction of the Madrid area (azimuth angle around 90 deg) are less than 20 dB.

In the direction from the Robledo DSN site to the city of Pozuelo de Alarcón (92 deg azimuth with respect to the north), there are two base stations deployed at a distance of 37.88 km. In this azimuth direction, the minimum elevation angle of the terrain seen by the

**Table 3. LMDS base station deployment around Madrid and elevation angles.**

City	No. of base stations	Approx. distance to DSN, km	Azimuth angle wrt DSN, deg	Min. ant. operating angle, deg	Terrain elev. angle, deg	Min. off-boresight angle, deg	Max. DSN Rec. Ant Gain, dB
Madrid	23	48.01	91	10	4.4	5.6	13.3
Alcobendas	1	53.52	76.4	10	5.8	4.2	16.4
Getafe	1	47.37	106.1	10	3.4	6.6	11.5
Majadahonda	1	32.37	79.1	10	6.7	3.3	19.0
Móstoles	1	34.10	108.8	10	3.4	6.6	11.5
Pozuelo de Alarcón	2	37.88	92	10	4.3	5.7	13.1
San Sebastián de los Reyes	1	54.45	77.8	10	6.4	3.6	18.1
Torrejón de Ardoz	1	65.03	87.2	10	6.8	3.2	19.4

DSN is 4.3 deg, and the separation angle is 5.7 deg. The receiving antenna gain in that direction is 13.1 dB and the corresponding minimum loss required is 168.7 dB. In this direction, the coordination distance from the DSN station is 10 km for 1.0 percent of time exceeded. It is fortunate that the existing stations deployed around Madrid are quite far away from the coordination area.

## VII. Conclusion

Based on the LMDS information provided by SETSI, we have performed a link analysis and propagation loss calculation to evaluate the interference effects on the DSN Robledo station. In order to protect the DSN receiving station from potential interference from LMDS operation in the 25.5- to 25.7-GHz band, we have defined a coordination zone around the Robledo DSN site for 1.0 percent of time exceeded as showed in Figures 8 and 9. Any LMDS stations within this zone could result in harmful interference to the DSN and should be avoided.

Based on the vendor's deployment pattern of LMDS stations around Madrid, we find that these stations are outside of the coordination area and hence will not exceed the allowed interference level established by the ITU. It can be concluded that the LMDS deployments currently conceived do not pose unacceptable interference to the DSN. It is suggested that any future deployment and addition of LMDS stations in this frequency band consider the coordination maps given in Figures 8 and 9.

It should be emphasized that the coordination area given in this report is based on the assumption that there is only one LMDS cell in each azimuth direction and that interference at that azimuth direction is totally from transmitters of this cell. If there is more than one LMDS cell in a given azimuth direction, the coordination area will be larger.

## **Acknowledgments**

The author would like to thank Miles Sue for his valuable advice in many aspects of this study, and Farzin Manshadi for his comments and suggestions on this paper.

## **Reference**

- [1] G. K. Noreen, R. J. Cesarone, L. J. Deutsch, C. D. Edwards, J. A. Soloff, T. Ely, B. M. Cook, David D. Morabito, H. Hemmati, Sabino Piazzola, R. Hastrup, D. S. Abraham, M. K. Sue, and F. Manshadi, "Integrated Network Architecture for Sustained Human and Robotic Exploration," paper no. 1378, *Proceedings of IEEE Aerospace Conference*, Big Sky, Montana, March 5–12, 2005.

## Appendix A

### Protection for Lagrangian Orbit Missions (Effects of a Lower System Noise Temperature on the Coordination Contour)

When the Robledo DSN station points its antenna to the Lagrangian points (or any deep space), instead of the Moon, the system noise temperature can be lowered from 350 K to ~100 K. Thus, the required minimum propagation loss to satisfy the ITU protection criteria will increase by 5.5 dB. This change will not significantly affect the shape of the coordination area defined in Figure 8. We still can use this coordination area for the protection of Lagrangian orbit missions or other deep space missions.

## Appendix B

### Percentage of Time Averaged Over a Lunar Track that the Protection Threshold Is Exceeded

In order to determine the average percentage of time when the protection criterion is exceeded, six (6) lunar passes (each separated by two months) were studied. The azimuth angle, the elevation angle, and the separation angle were first calculated as a function of time during the track by performing a computer simulation using the Satellite Orbit Analysis Program (SOAP). The effective receive antenna gain and the required minimum loss as a function of time were then computed. Using the required loss determined by the coordination contour in Figure 8 (which is for  $p = 1.0$  percent and a minimum operating angle of 10 degrees) as a reference, the percent of time at time instance  $t_i$  during the track,  $p(t_i)$  is estimated by comparing the required loss at that time instance to the reference loss. The percentages  $\{p(t_i), i = 1, 2, \dots, n\}$  during the track are then used to determine the average percentage of time for that track. Tables B1 through B6 show the calculations for the six tracks studied. From these tables, we can see that, above the 10-deg elevation angle (operating limit), as the elevation angle increases, the separation (off-axis) angle also increases. Therefore, the receiving antenna gain rapidly decreases, hence requiring a small propagation loss (as shown in Equation 3), which in turn corresponds to a smaller percentage of time. As shown in the tables, the average percentage of time is very small ( $< 0.02$  percent) for the six tracking passes examined.

**Table B1. Geometry and probability of interference for Case 1.**

Tracking Time 1/1/2005 UTC	Azimuth Angle	Elevation Angle	Separation Angle	Off-Axis Gain	Min. Loss Required	Percent of Time Exceeded
22:38:00	83.4957	10.0199	2.8716	20.82	176.40	1.00000
22:39:00	83.652	10.2018	3.0268	20.07	175.65	0.42170
22:40:00	83.8084	10.3839	3.1924	20.07	175.65	0.42170
22:41:00	83.9648	10.566	3.3669	19.37	174.95	0.18836
22:42:00	84.1213	10.7482	3.549	18.71	174.29	0.08810
22:43:00	84.2778	10.9304	3.7375	18.09	173.67	0.04315
22:44:00	84.4343	11.1127	3.9316	17.51	173.08	0.02188
22:45:00	84.5909	11.295	4.1304	16.95	172.53	0.01161
22:46:00	84.7476	11.4774	4.3333	16.42	172.00	0.00631
22:47:00	84.9043	11.6599	4.5398	15.91	171.49	0.00351
22:48:00	85.0611	11.8424	4.7494	15.43	171.01	0.00202
22:49:00	85.2179	12.025	4.9617	14.97	170.55	0.00119
22:50:00	85.3748	12.2076	5.1764	14.53	170.10	0.00071
.....	.....	.....	.....	.....	.....	.....
04:28:00	178.5600	59.7722	86.0326	-10.00	145.58	0.00000
04:29:00	179.0411	59.7723	86.2725	-10.00	145.58	0.00000
Average						0.00630

**Table B2. Geometry and probability of interference exceeded for Case 2.**

Tracking Time 3/1/2005 UTC	Azimuth Angle	Elevation Angle	Separation Angle	Off-Axis Gain	Min. Loss Required	Percent of Time Exceeded
23:51:00	120.3404	10.1106	7.2245	10.57	165.99	1.00000
23:52:00	120.5185	10.2671	7.3721	10.57	165.99	1.00000
23:53:00	120.6969	10.4234	7.524	10.27	165.70	0.71614
23:54:00	120.8758	10.5793	7.6797	9.98	165.41	0.51286
23:55:00	121.055	10.735	7.8393	9.70	165.13	0.37154
23:56:00	121.2345	10.8903	8.0023	9.42	164.85	0.26915
23:57:00	121.4145	11.0454	8.1687	9.42	164.85	0.26915
23:58:00	121.5948	11.2002	8.3381	9.15	164.58	0.19724
23:59:00	121.7755	11.3546	8.5105	8.89	164.32	0.14622
00:00:00	121.9565	11.5088	8.6856	8.64	164.06	0.10839
00:01:00	122.138	11.6626	8.8633	8.39	163.82	0.08222
00:02:00	122.3198	11.8162	9.0434	8.14	163.57	0.06166
00:03:00	122.502	11.9694	9.2258	7.91	163.33	0.04677
.....	.....	.....	.....	.....	.....	.....
03:59:00	178.7733	33.1612	61.8722	-10.00	145.58	0.00000
04:40:00	179.0544	33.1611	62.0981	-10.00	145.58	0.00000
Average						0.01654

**Table B3. Geometry and probability of interference exceeded for Case 3.**

Tracking Time 5/1/2005 UTC	Azimuth Angle	Elevation Angle	Separation Angle	Off-Axis Gain	Min. Loss Required	Percent of Time Exceeded
03:09:00	133.4331	10.1128	6.3311	12.19	167.80	1.00000
03:10:00	133.6122	10.2484	6.4555	11.85	167.46	0.67608
03:11:00	133.7916	10.3835	6.5847	11.85	167.46	0.67608
03:12:00	133.9715	10.5183	6.7186	11.51	167.12	0.45709
03:13:00	134.1517	10.6528	6.8567	11.19	166.80	0.31623
03:14:00	134.3324	10.7868	6.9988	11.19	166.80	0.31623
03:15:00	134.5134	10.9204	7.1448	10.87	166.48	0.21878
03:16:00	134.6949	11.0536	7.2943	10.57	166.18	0.15488
03:17:00	134.8767	11.1865	7.4472	10.27	165.88	0.10965
03:18:00	135.059	11.3189	7.6032	9.98	165.59	0.07852
03:19:00	135.2416	11.4509	7.7623	9.98	165.59	0.07852
03:20:00	135.4247	11.5825	7.9241	9.70	165.31	0.05689
03:21:00	135.6082	11.7137	8.0885	9.42	165.03	0.04121
.....	.....	.....	.....	.....	.....	.....
06:43:00	180.8361	26.4576	50.2407	-10.00	145.58	0.00000
06:44:00	181.0867	26.4577	50.4537	-10.00	145.58	0.00000
Average						0.01944

**Table B4. Moon track geometry and probability of interference exceeded for Case 4.**

Tracking Time 7/1/2005 UTC	Azimuth Angle	Elevation Angle	Separation Angle	Off-Axis Gain	Min. Loss Required	Percent of Time Exceeded
02:04:00	78.7956	10.0002	3.3459	19.37	174.60	1.00000
02:05:00	78.9427	10.1839	3.5074	18.71	173.94	0.46774
02:06:00	79.0898	10.3677	3.6769	18.09	173.32	0.22909
02:07:00	79.237	10.5516	3.8533	17.51	172.73	0.11614
02:08:00	79.384	10.7356	4.0357	16.95	172.18	0.06166
02:09:00	79.5311	10.9196	4.2233	16.42	171.65	0.03350
02:10:00	79.6781	11.1038	4.4156	15.91	171.14	0.01862
02:11:00	79.8252	11.2881	4.6118	15.43	170.66	0.01072
02:12:00	79.9722	11.4724	4.8116	14.97	170.20	0.00631
02:13:00	80.1192	11.6569	5.0144	14.53	169.75	0.00376
02:14:00	80.2662	11.8414	5.22	14.10	169.33	0.00232
02:15:00	80.4132	12.026	5.428	13.69	168.92	0.00145
02:16:00	80.5602	12.2108	5.6382	13.30	168.52	0.00091
.....	.....	.....	.....	.....	.....	.....
08:13:00	181.3222	66.0704	88.6993	-10.00	145.58	0.00000
08:14:00	181.902	66.0686	88.9281	-10.00	145.58	0.00000
Average						0.00528

**Table B5. Geometry and probability of interference exceeded for Case 5.**

Tracking Time 9/1/2005 UTC	Azimuth Angle	Elevation Angle	Separation Angle	Off-Axis Gain	Min. Loss Required	Percent of Time Exceeded
04:14:00	70.1206	10.0402	5.5779	13.69	169.10	1.00000
04:15:00	70.2675	10.2126	5.7346	13.30	168.71	0.63826
04:16:00	70.4143	10.3851	5.8959	12.91	168.32	0.40738
04:17:00	70.5609	10.5578	6.0615	12.55	167.96	0.26915
04:18:00	70.7075	10.7307	6.2311	12.19	167.60	0.17783
04:19:00	70.854	10.9038	6.4043	11.85	167.26	0.12023
04:20:00	71.0004	11.077	6.5808	11.85	167.26	0.12023
04:21:00	71.1467	11.2503	6.7605	11.51	166.92	0.08128
04:22:00	71.2929	11.4239	6.943	11.19	166.60	0.05623
04:23:00	71.439	11.5976	7.1281	10.87	166.28	0.03890
04:24:00	71.5851	11.7714	7.3157	10.57	165.98	0.02754
04:25:00	71.731	11.9454	7.5056	10.27	165.68	0.01950
04:26:00	71.8769	12.1196	7.6975	9.98	165.39	0.01396
.....	.....	.....	.....	.....	.....	.....
10:44:00	180.1249	70.3545	92.1306	-10.00	145.58	0.00000
10:45:00	180.8077	70.3501	92.3477	-10.00	145.58	0.00000
Average						0.00760

**Table B6. Geometry and probability of interference exceeded for Case 6.**

Tracking Time 11/1/2005 UTC	Azimuth Angle	Elevation Angle	Separation Angle	Off-Axis Gain	Min. Loss Required	Percent of Time Exceeded
07:10:00	117.4441	10.0624	7.177	10.87	166.30	1.00000
07:11:00	117.6209	10.2236	7.329	10.57	165.99	0.69984
07:12:00	117.798	10.3845	7.4853	10.27	165.70	0.50119
07:13:00	117.9755	10.5452	7.6455	9.98	165.41	0.35892
07:14:00	118.1534	10.7056	7.8095	9.70	165.13	0.26002
07:15:00	118.3316	10.8658	7.977	9.70	165.13	0.26002
07:16:00	118.5101	11.0256	8.1477	9.42	164.85	0.18836
07:17:00	118.689	11.1852	8.3215	9.15	164.58	0.13804
07:18:00	118.8683	11.3446	8.4983	8.89	164.32	0.10233
07:19:00	119.0479	11.5036	8.6777	8.64	164.06	0.07586
07:20:00	119.2279	11.6624	8.8597	8.39	163.82	0.05754
07:21:00	119.4083	11.8209	9.0441	8.14	163.57	0.04315
07:22:00	119.5891	11.9791	9.2307	7.91	163.33	0.03273
.....	.....	.....	.....	.....	.....	.....
11:28:00	179.1317	35.0208	64.9574	-10.00	145.58	0.00000
11:29:00	179.4220	35.0193	65.1866	-10.00	145.58	0.00000
Average						0.01436